



Development and assessment of polyacrylamide-starch hydrogel nanocomposites with graphene quantum dots for targeted quercetin delivery to brain tumors

Pardis Ordoukhani ^a, Mehrab Pourmadadi ^{b,*}, Majid Abdouss ^{a,*}

^a Chemistry Department, Amirkabir University of Technology, Tehran, Iran

^b Protein Research Center, Shahid Beheshti University, Tehran, GC, 1983963113, Iran

ARTICLE INFO

Keywords:

Polyacrylamide
Starch
Graphene quantum dots
Quercetin
Drug delivery systems
Controlled release
Brain cancer

ABSTRACT

Brain carcinoma remains among the most challenging cancers to treat due to the restrictive blood-brain barrier (BBB), which limits drug bioavailability and durability. Quercetin (QC), a natural polyphenol with strong anticancer effects, suffers from poor BBB permeability. In this research, an innovative pH-sensitive hydrogel nanocomposite was engineered via physical cross-linking using a novel combination of polyacrylamide (PAM), starch (S), and graphene quantum dots (GQDs), serving as a promising nanocarrier for enhanced QC delivery. The uniqueness of this work lies in the synergistic integration of these specific materials through a newly implemented double emulsion method (W/O/W), enabling targeted, stable, and biocompatible drug transport across the BBB. The nanocomposite achieved exceptional encapsulation efficiency (EE) and loading efficiency (LE) of 89 % and 48 %, respectively—among the highest reported. Fourier transform infrared (FTIR) spectroscopy, Field emission scanning electron microscopy (FE-SEM), and X-ray diffraction (XRD) analyses confirmed strong molecular interactions, favorable semi-globular nanoparticle morphology, and a mostly amorphous structure, respectively. The nanoparticles (NPs) exhibited an optimal size range of 42.68–58 nm with a low Polydispersity Index (PDI) of 0.28, indicating excellent dispersion. Dynamic light scattering (DLS) and zeta potential analysis (average: +53.3 mV) revealed high colloidal stability. Drug release was 46 % higher in tumor-simulated conditions after 96 h, reflecting targeted delivery potential. MTT assays on L929 (normal cells) and U-87 MG (cancerous cells) cell lines confirmed significant biocompatibility, with the QC-loaded nanocomposite showing 13 % reduced cytotoxicity compared to free QC on the L929 cell line. These findings support the potential of the developed nanocarrier as an efficient and targeted drug delivery platform for brain tumor therapy.

1. Introduction

The battle against cancer, the second-leading cause of mortality, presents numerous challenges for researchers. One of the world's top causes of death, cancer, shortens life expectancy (Siegel, Miller, Wagle & Jemal, 2023; Sung et al., 2021). A rare kind of cancer that affects people of all ages, cancerous primary brain and central nervous system (CNS) malignancies have a high fatality and morbidity rate (Zhang et al., 2017). Between the years 2007 and 2011, the median annual age-adjusted occurrence prevalence of brain cancers across the United States was 7.25 per 100,000 people (Ostrom et al., 2014). Even though brain cancer is becoming more common, treatment for these diseases is fraught with difficulties. The majority of medication protocols for brain

cancer focus on radiation therapy after surgery, which is intrusive and has a short average survival time of fewer than two years (Nance, Pun, Saigal & Sellers, 2022).

Glioblastoma multiforme (GBM) is recognized as one of the most aggressive and deadliest tumors affecting the CNS, accounting for nearly half of all brain malignancies. Despite decades of clinical and scientific effort, including surgical removal combined with radiotherapy and chemotherapy, patient outcomes remain dismal. The complexity of GBM lies in its cellular diversity, invasive growth pattern, and limited responsiveness to conventional treatments. In particular, the presence of drug-resistant cancer cell subpopulations, diffuse tumor spread into normal brain tissue, and the stimulation of glioma stem cells following surgery significantly reduce treatment efficacy. Additionally, the blood-

* Corresponding authors.

E-mail addresses: pardisordoukhani2001@gmail.com (P. Ordoukhani), mehrabpourmadadi@gmail.com (M. Pourmadadi), phdabdouss44@aut.ac.ir (M. Abdouss).

brain barrier (BBB) severely restricts the penetration of most therapeutic compounds, especially those exceeding 400 Da in molecular weight. These biological barriers contribute to a median survival time of just over one year, with long-term survival beyond five years occurring in <5 % of patients. Such challenges underscore the urgent need for novel therapeutic strategies and advanced drug delivery systems capable of overcoming the BBB and selectively targeting GBM cells (Nozhat et al., 2024).

Chemotherapy is an extensively used treatment that aims to slow down or stop the fast growth of tumor cells, but it frequently causes harm to normal cells as well, which can result in a variety of unwanted side effects. Radiotherapy is a different approach that damages malignant cells but is not precise enough to avoid harming nearby normal cells, which might lead to nutritional issues. For a long time, finding a type of cancer therapy plan that eliminates side effects, financial strains, and disturbance to daily life has been a difficult clinical task (M. Najafi et al., 2024). As a result, researchers have adopted novel approaches based on nanotechnology. The science of nanotechnology is increasingly recognized in various medical fields, especially in the prevention and therapy of cancer. By utilizing the power of nanoparticles (NPs) and developing innovative methods for targeted drug delivery (TDD), this advanced technology has completely changed the examination and therapy of diseases (Arcos & Vallet-Regi, 2013).

The scarcity of viable cancer therapy options, particularly for brain tumors, emphasizes the bleak nature of the condition. These tumors exhibit resistance to both traditional and advanced therapies as a result of their distinctive characteristics, which highlights the need for continuous investigation into innovative treatment methods (Shah & Kochar, 2018; Miller et al., 2021; Khodayari, Heydarinasab, Moniri & Miralinaghi, 2023). The BBB, which is made up of tight connections between endothelial cells and many medications and macromolecules that can't pass through it, also limits the amount of drug that can be delivered to the brain (Power et al., 2022; Lesniak & Brem, 2004). Bioactive chemicals have garnered significant interest as a natural cancer treatment among many medications (Atanasov, Zotchev, Dirsch & Supuran, 2021; Saeed, Khan & Shabbir, 2012; Almatroodi et al., 2022). More work has been done to make new medicines easier to dissolve and absorb, like quercetin (QC), which has the disadvantages of being hydrophobic and not dissolving easily. This makes it hard for the body to absorb (Ahmadi et al., 2023; Ishisaka et al., 2011; Caro et al., 2022; Azeem et al., 2023; Nathiya, Durga & Devasena, 2014).

Quercetin is one of the flavonoid chemicals present in a wide variety of edible and medicinal plants. For the purpose of treating brain tumors, QC exhibits great promise in the role of neuro-inflammatory inhibitor and an antioxidant drug (Shala, Arduino, Salihu & Denora, 2023). Due to its effective blood-brain barrier crossing, it demonstrates neuro-protective effects despite having poor bioavailability (Ghasemizadeh et al., 2023). pH-sensitive TDD with hydrogels is one method of medication delivery for cancer cells. There is promise for utilizing polymers with a higher cargo release rate during an acidic condition compared to an alkaline one because malignant cells experience an acidic environment due to oncogenic metabolism, which makes them more acidic than normal cells (Li, Huang & Wu, 2021; Pourmadadi et al., 2023). For the transport of QC, several nanocarriers have been developed and produced. Najafi et al. (M. Najafi et al., 2024) with an emphasis on the cell line HepG2, researchers aimed to investigate the effect of QC-loaded nanocarriers on causing apoptosis (planned cell death) in liver cancerous cells. Investigators added GQDs to Aga/α-Fe2O3 nanocomposites to improve the effectiveness of drug administration further. Also, Ahmadi et al. (Ahmadi et al., 2023) effectively employed a PAA/Aga/ZnONPs nanocarrier to carry QC to the target organ for curing breast carcinoma. The proliferation of MCF7 breast cancer cells was efficiently impeded by the nontoxic ZnO@QC composite.

Large volumes of water may be retained by hydrogels, which are three-dimensional networks of cross-linked hydrophilic polymers (Vyas & Khar, 2004; Peppas, 1986; Brannon-Peppas & Harland, 2012).

Hydrogels have a long history of usage in the biomedical field for a variety of purposes, including drug delivery systems (DDSs), super-absorbents, soft contact lenses, and wound dressings (Peppas, 1986; Tsuruta, 1993; Ratner, 1976; Peppas & Langer, 1994; Narasimhan, Peppas & Park, 1997; Peppas, 1997). One synthetic polymer that is frequently utilized in the creation of hydrogels is polyacrylamide (PAM), which has good hydrophilicity and is non-toxic (Kandow, Georges, Janmey & Beningo, 2007). Generally, ammonium persulfate (APS) is used in the role of activator while N,N,N',N'-tetramethyl ethylene diamine (TEMED) is applied as a catalyst (AAm) to polymerize AAm with N,N'-methylene bisacrylamide (MBA) for a dual-functional crosslinking reagent to generate PAAm hydrogels (Su, Mahalingam, Edirisinha & Chen, 2017). However, because PAM is soft and lacks an energy dissipation mechanism, the covalently crosslinked PAM-based hydrogels are often brittle (Lin, Ma, Wang & Zhou, 2015). Methods based on the combination of several mechanisms or non-covalent crosslinking have been used to enhance the mechanical performance of the PAM hydrogel. Hydrogels created via hydrophobic crosslinking have been shown to have exceptional fatigue resistance and great toughness (Haque, Kurokawa, Kamita & Gong, 2011).

Starch (S) is an endogenous polymer found in several green plants (Builders & Arhewoh, 2016). With the potential for use in medicine, starch is the third most prevalent biopolymer. It is mostly composed of two molecules, amylose (75–85 %) and amylopectin (15–25 %), with trace amounts of protein and other components (Avval, Moghaddam & Fareghi, 2013). The non-toxic and non-irritant characteristics, together with its low cost, simplicity of modification, and variety in use, have positioned starch as a very prominent polymer utilized as a pharmaceutical excipient (Builders & Arhewoh, 2016). Because of its cross-linkable characteristics, which enable it to spontaneously degrade into molecules that are acceptable to the body, it is utilized to make NPs for DDSs. This eliminates the requirement for removal after drug administration (Zhang et al., 2013; Sujka et al., 2018). Very few studies have explored the use of PAM and starch together to create composite hydrogels. The majority of earlier papers dealt with grafting reactions to create copolymers, which were then employed to create multicomponent networks (Elvira, Mano, San Roman & Reis, 2002; Shaik et al., 2013; Murthy, Mohan, Seeramulu & Raju, 2006; Parvathy & Jyothi, 2012).

In recent work, Murthy et al. (Murthy, Mohan, Seeramulu & Raju, 2006) to assess the expanding and dissemination properties of materials in simulated biological liquids, they developed semi-interpenetrating polymer networks (IPN) hydrogels made of starch and an accidental mixture of poly(acrylamide-co-sodium methacrylate). The performance of biomaterials for pharmaceutical applications was deemed by the authors to be promising (Torres-Figueroa et al., 2020). Their results showed excellent gel-forming ability and amazing biocompatibility, resulting in a stable gel within the body. According to this study, PAM/Starch hydrogel has the potential to be used as a hydrogel-composite for multiple biological fields. Due to several publications, carbon or NPs made from it are used in the fields of biotechnology (Jokandan et al., 2019; RezaeiKalantary et al., 2014; Azari, Nabizadeh, Mahvi & Nasser, 2022). Graphene, one of the carbon-based NPs, has demonstrated superior qualities for drug delivery applications, including enhancing therapeutic benefits and boosting delivery efficiency (Kazemi, Pourmadadi, Yazdian & Ghadami, 2021; Parvaneh et al., 2023; Rahmani et al., 2022; Zoghi et al., 2023; Goenka, Sant & Sant, 2014).

Graphene quantum dots (GQDs) represent an innovative category of graphene-derived nanomaterials, characterized by sheets that may consist of one or multiple layers and possess a width of <100 nm (Zadeh et al., 2023). Extensive literature has revealed that GQDs have intrinsic fluorescent characteristics, excellent dispersion in water, little toxicity, consistent photoluminescence (PL), and favorable biocompatibility. Lastly, their exceptional ability to resist photobleaching renders them valuable multifunctional materials for the chemical and medicinal

industries. With no surface functionalization or passivation, GQDs have a quasi-zero-dimensional structure and atomic layers that give them strong PL (Iannazzo, Celesti & Espro, 2021). To visualize malignant tumors, GQD offers a special feature that can greatly increase signals. GQDs have been extensively studied for their use as multipurpose transmitters for malignant tumor monitoring and therapy, as well as for photothermal therapy (PTT), photodynamic therapy (PDT), and guided multimodal imaging (Tade & Patil, 2020). Incorporating GQDs within drug delivery systems for the treatment of cancer may improve and speed up the DNA-destroying impact due to their advantageous physicochemical characteristics (Wang et al., 2013; Iannazzo et al., 2017).

To illustrate, in research by Ostovar et al. (Ostovar, Pourmadadi & Zaker, 2023) the researchers utilized GQDs to functionalize chitosan (CS) and carboxymethylcellulose (CMC) to release the ZnO@QC for brain tumor therapy. They also added GQDs to improve the mechanical and chemical resistance of CS/CMC. Additionally, their results showed that 49 % of tumor boundaries were observed after examination of in vitro cell death, demonstrating the applicability of their techniques for usage in medication administration. The blood-brain barrier (BBB) permeability of GQDs is one of their key characteristics. Molecules <40 Da and lipid soluble can pass the BBB. GQDs can passively diffuse or use glucose transporter proteins to traverse the BBB. Their tiny size and surface function allow for facile BBB penetration, which aids in TDD to the brain. GQDs by themselves have demonstrated efficacy in the management and prophylaxis of nervous system disorders (Henna & Pramod, 2020). To prevent and cure Alzheimer's disease, for instance, amyloid- β buildup is successfully inhibited by GQDs' covalent interaction with tramiprosate (Liu et al., 2015; Liu et al., 2017).

In this study, we describe a new drug delivery system made of four parts, created using a unique method called dual-phase emulsion (W/O/W), which includes PAM, starch, GQDs, and QC. This is, to the best of our knowledge, the first time anyone has combined these four components into one system to see how GQDs influence the pH-sensitivity of the PAM/Starch hydrogel to deliver the QC antitumor drug. Beyond its novel composition, the system exhibits a compelling set of properties, including remarkable biocompatibility, negligible cytotoxicity, high drug-loading efficiency, and robust structural integrity. The deliberate synergy among the selected materials enables enhanced drug release control and potentially improved therapeutic efficacy. These unique characteristics collectively position this platform as a promising and unprecedented advancement in the field of drug delivery. To make the PAM/Starch/GQDs hydrogel nanocomposite, GQDs were mixed into the PAM/Starch solution. The next step involved injecting PAM/Starch/GQDs coated with SPAN 80 surfactant into a hydrophobic oil phase to form spherical drug nanocarriers. By employing the w/o/w emulsification method, nanocarriers were produced. The relationships between the components of the nanocomposite were assessed using Fourier transform infrared (FTIR) analysis. The morphology of the nanocarriers was analyzed through field emission scanning electron microscopy (FE-SEM), while the crystalline or amorphous nature of their structures was examined using X-ray diffraction (XRD). Ultimately, the method known as MTT has been used for evaluating biological compatibility and anti-cancer characteristics of PAM/Starch/GQDs@QC nanocomposites by using L929 and U-87 MG cell lines.

2. Materials and methodology

2.1. Materials

Polyacrylamide (PAM, $(\text{C}_3\text{H}_5\text{NO})_n$, Mw = 150 kDa), starch ($\text{C}_6\text{H}_{10}\text{O}_5$)_n, citric acid, acetic acid (99.5 %), and Span 80 (molar mass = 428.60 g/mol) were acquired from the Merck Corporation. (Germany). Quercetin medication (>95 % (HPLC), Dialysis bag (12Kd and 7Kd cut off), MTT powder, phosphate buffer saline (PBS, pH 7.4), and Fetal bovine serum (FBS) were also provided by Sigma Aldrich Co. (USA). The Pasteur Institute in Iran provided us with the human cancerous cell glioblastoma

(U-87 MG) and mouse fibroblast cell line (L929).

2.2. Fabrication of GQDs

To undergo a transformation, we heat 10 g of citric acid at a temperature of 200 °C for about 5 min. Upon the completion of that procedure, the resultant yellow liquid experiences a transition in hue to orange shortly after a duration of 30 min, indicating the development of GQDs (Ostovar, Pourmadadi & Zaker, 2023).

2.3. Fabrication of PAM/Starch/GQDs hydrogel-nanocomposites and loading of QC

During the first phase, to create a homogeneous hydrogel containing 2 % v/w PAM, mix 40 ml of 2 % v/v acetic acid solution at ambient temperature with 0.8 g of powdered PAM using a thermal stirrer. The hydrogel created in the previous step should be well mixed with 0.4 g of starch powder until it dissolves entirely before being treated for 10 min in an ultrasonic bath. Stir the above solution until it becomes uniform on the heater stirrer after adding 40 mg of previously produced GQDs nanoparticles (M. Najafi et al., 2024). The next step is to apply enough QC into the hydrogel nanocomposites until the final drug dosage is 1 mg/ml. After 30 min on a thermal stirrer, the hydrogel becomes a one-handed PAM/Starch/GQDs hydrogel containing QC drug (Eshaghi, Pourmadadi, Rahdar & Díez-Pascual, 2022).

2.4. Synthesis of double-emulsion-encapsulated pam/starch/gqds@qc nanocarrier

In the following stage, the one-handed PAM/Starch/GQDs@QC hydrogel should be prepared in a 20 mL volume utilizing a syringe and added gradually into the water-repellent phase. The water-repellent phase (60 mL of hazelnut oil containing 2 % v/v SPAN 80 as surfactant) has to be stirred. In order to reduce the size of the nanocarrier into the water-repellent phase and obtain a spherical and homogeneous shape, vigorously mix the solution on the heater stirrer. 60 mL of deionized water has been used as the water-repellent phase for the gradual wash after 10 min. Following 30 min, by removing the mixture out of the heater stirrer, the layers were left to develop for approximately 15 min. Then, using a sampler, gather the oil phase. Next, the watery phase was removed from the PAM/Starch/GQDs@QC nanocarrier by centrifuging it for 10 min at 6000 rpm. A lyophilizer is used to crush all the samples into different sizes. It is placed in the refrigerator at -20 °C until it completely freezes, and then they're freeze-dried (M. Najafi et al., 2024; Ostovar, Pourmadadi, Shamsabadipour & Mashayekh, 2023).

2.5. Characterization of nanoparticles (NPs)

Several analytical studies were conducted on the nanocomposite and nanocarrier to comprehend their features and qualities. Numerous functional groups within the mixture were identified through Fourier transform infrared spectroscopy (FTIR), which was also utilized to evaluate the connections between each sample's constituent parts. FTIR analysis was carried out by applying software loaded on a PerkinElmer Spectrum One spectrophotometer (Versioning 10.03.06). The nanocarrier's structural characteristics and crystallinity were investigated using X-ray diffraction (XRD) analysis in the 2θ range between 10 and 80°, utilizing a PAN analytical xPert pro crystal diffractometer. The NPs' morphology was studied through field emission scanning electron microscopy, operating at 20 kV and using an appropriate magnification (FESEM: TESCAN, MIRA3, Czech). The dynamic light scattering (DLS) technique (Instruments Malvern, United Kingdom) was employed to investigate the surface charge of nanocarriers and their average size. By measuring the amount of reflected light by tiny particles within a sample, DLS offers important information about how their sizes are

distributed. To assess the zeta potential (Horiba SZ-100), the dispersion's pH was kept between 7.2 and 7.4.

2.6. Assessment of medication loading (LE %) and encapsulation efficiency (EE %)

Following exact measurement, 1 mL of phosphate-buffered solution (PBS) along with 1 mL of ethyl acetate was added to 1 mg of the PAM/Starch/GQDs nanocomposite. The combination was subsequently stirred to separate the ethyl acetate layer. Drug release may be accomplished by isolating the ethyl acetate layer (Ostovar, Pourmadadi & Zaker, 2023). A UV-Vis optical spectrometer operated at 370 nm was utilized to measure the quantity of free QC, and the results showed an obvious density correlation of light and the quantity of free medication in this phase of the process. To calculate the proportion of QC encapsulation efficiency (EE) and medication loading (LE), Eqs. (1) and (2) were applied (Eshaghi, Pourmadadi, Rahdar & Díez-Pascual, 2022).

$$\text{EE} (\%) = \frac{[(\text{Total value of QC}) - (\text{Free value of QC})]}{(\text{Total value of QC})} \times 100 \quad (1)$$

$$\text{LE} (\%) = \frac{[(\text{Total value of QC}) - (\text{Free value of QC})]}{(\text{Total value of Nanocomposite})} \times 100 \quad (2)$$

2.7. Investigation of drug release in laboratory environments

Utilizing PBS solution around pH 7.4 and 5.4, which correspond to the acidity of malignant cells and the natural pH of normal cells, the QC discharge properties of the PAM/Starch / GQDs hydrogel nanocomposite were determined. The dialysis technique was employed to evaluate the release kinetics (Luo et al., 2010). Afterwards, the nanocarriers were soaked in a dialysis container (molecular weight threshold of 12 kDa) at 37 °C, and 1 ml of them was immersed in 15 ml of PBS. Using fresh buffer, 300 µl of each sample was removed at predetermined times (0, 0.5, 1, 2, 3, 6, 12, 24, 48, 72, and 96 h) and substituted with the original media in the same quantity. Drugs have been dispersed with the aid of a spectrophotometer set to 370 nm, and the estimated quantity of QC liberated was determined following the (3) equation (Pourmadadi, Ahmadi & Yazdian, 2023).

$$\text{Percentage of QC released} (\%) = \frac{(\text{QC released})}{(\text{QC loaded})} \times 100 \quad (3)$$

Eq. (3) is an essential element in comprehending the liberation study. Loaded QC refers to the initial dosage of medication included in the NPs. In contrast, Released QC describes the amount of drug in the samples that were extracted as determined by a UV-visible spectrophotometer (Pourmadadi et al., 2024).

2.8. Supplying cell cultures and evaluating in vitro cytotoxicity analysis

Utilizing the MTT test, the formulations' potential cytotoxic effects on malignant glioma cells in humans (U-87 MG) and non-cancerous (L929) cells were evaluated. The cultured cells were transferred to plates with 96 wells and incubated for 48 h. Next, the control cells were grown for another 72 h. The fundamental solution (DMEM) contains 1% antibiotic (penicillin/streptomycin) and 10 % FBS, which was divided into individual wells. After a 4-hour incubation period, 50 µL of 5 mg/mL MTT was placed into every well in combination with the produced nanocomposite (PAM/Starch/GQDs@QC) and free QC. Subsequently, DMSO was used to dissolve the formazan crystals. The light absorbance of the dissolved formazan derivatives was analyzed by applying a microplate reader determined around 570 nm. Furthermore, the same processes have been applied to normal cells. In the end, through Eq. (4), the viability percentage was determined (M. Najafi et al., 2024).

$$\text{cell viability} (\%) = \frac{[\text{Absorbance}]_{\text{samples}}}{[\text{Absorbance}]_{\text{control sample}}} \times 100 \quad (4)$$

3. Findings and analysis

3.1. FTIR assessment

The presence of each element in the nanocomposite was established using Fourier Transform Infrared Spectroscopy (FTIR) by analyzing the observed peaks that suggested connections among polyacrylamide (PAM), Starch (S), graphene quantum dots (GQDs), and quercetin (QC) as the model drug. Because of the N-H stretching vibration of the NH₂ group and the C-H stretching vibrations, the PAM spectra (Fig. 1a) reveal two bands at 3438 and 2928 cm⁻¹. Stretching of the C=O group and CH₂ scissoring in amide, accordingly, is responsible for the bands at 1637 and 1456 cm⁻¹ (Singh & Mahto, 2017). According to earlier research on native starch structure, the wide peak in the spectrum of Starch (Fig. 1b) around 3000–3440 cm⁻¹ belongs to O—H stretching vibrations, but the highest point about 2900 cm⁻¹ relates to C—H stretching vibrations. Starch exhibits CO bond stretching vibration when peaks around 1150 and 927 cm⁻¹ are observed. The anhydrous glucose ring O—C stretching can be recognized by the characteristic peaks around 1080 cm⁻¹ and 1016 cm⁻¹ (M. Najafi et al., 2024). The peaks at approximately 3263–3632 cm⁻¹ in the PAM/Starch spectrum (Fig. 1c) are attributed to the overlapping of the O—H stretching band of the starch's hydroxyl groups and the N—H stretching band of the amide groups of acrylamide. C—H stretching vibrations of the methylene group and C—O—C stretching vibrations are responsible for the minor peaks around 2930.15 cm⁻¹ and 929.23 cm⁻¹. Importantly, the PAM/Starch signals show a lower wavenumber (1456 cm⁻¹) for the band approximately at 1466 cm⁻¹ which corresponds to the NH₂ bending vibration of PAM. This indicates that there may be some physical interactions between the two components, such as hydrogen bonding. One can ascribe a mighty peak near 1382.78 cm⁻¹ to C—N stretching. The hydrogelation procedure is confirmed by the emergence of these additional peaks in PAM/Starch as opposed to Starch (Torres-Figueroa et al., 2020; Setty, Deshmukh & Badiger, 2014).

Concerning the GQDs spectrum (Fig. 1d), the existence of O—H stretching vibrations ascribed by the exterior hydroxyl groups was indicated by peaks in the graphene quantum dots' FTIR spectra that were found at approximately 3440 cm⁻¹. The carbon-based structure's C—H stretching vibrations in aromatic rings were linked to peaks about 2854–2924 cm⁻¹, whereas a skeletal resonance of aromatic rings is situated between 1726 and 1404 cm⁻¹ (Ostovar, Pourmadadi & Zaker, 2023). Different peaks from each component may be seen in the PAM/Starch/GQDs spectra (Fig. 1e). The O—H stretching, C—H stretching, and C=O stretching vibrations are linked to the peaks that are visible at 3440 cm⁻¹, 2926 cm⁻¹, and 1650–1750 cm⁻¹, respectively. The shift in these carbonyl peaks points to possible hydrogen bonding-based interactions between PAM and Starch within the composite. The spectrum probably still shows peaks related to PAM/Starch/GQDs, notably those around 3400 cm⁻¹ and 1600 cm⁻¹, suggesting that PAM/Starch/GQDs are still present in the nanocomposite. PAM/Starch/GQDs@QC's FTIR spectrum (Fig. 1f) can display extra peaks linked to the flavonoid component quercetin (QC). According to the loading of QC and interactions inside the nanocarrier, these peaks may be associated with O—H stretching vibrations, C—H stretching vibrations, and some functional groups observed in QC (M. Najafi et al., 2024). Ultimately, the FTIR spectrum comparison shows that the constructed nanocarrier system included every component of the nanocomposite. Furthermore, it was verified how the quercetin drug interacted with the other materials as well as with them.

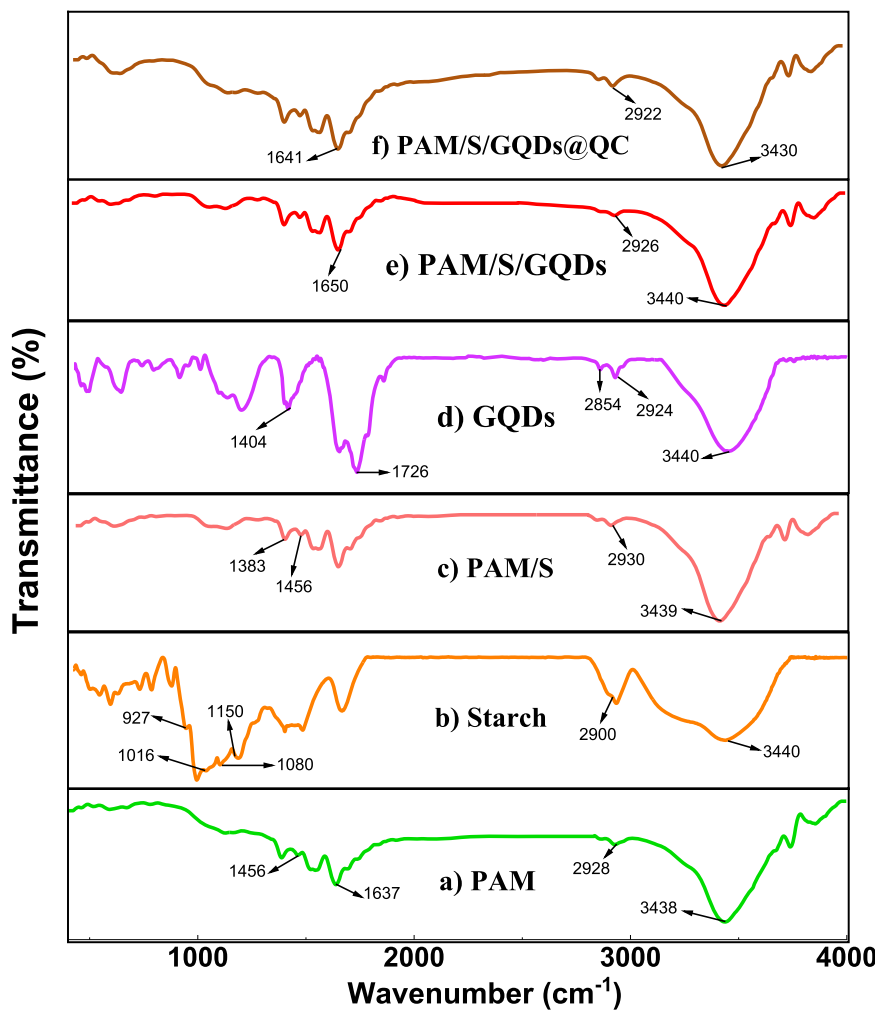


Fig. 1. An assortment of instances' FT-IR absorption spectra were gathered, containing: a) PAM, b) Starch, c) PAM/Starch, d) GQDs, e) PAM/Starch/GQDs nanocomposite, and f) PAM/Starch/GQDs@QC nanocarrier.

3.2. XRD assessment

The crystallinity of PAM/Starch/GQDs@QC and its components was investigated through X-ray diffraction analysis. According to the XRD data in Fig. 2a, PAM is characterized by the development of an amorphous material. It is evident from XRD profiles that PAM has an amorphous structure; an extensive peak emerged around $2\theta = 25^\circ$ (Moulay et al., 2013). The two main components of starch, amylopectin and amylose, indicate that it is a semi-crystalline substance that has both crystalline and amorphous features. To demonstrate its semi-crystalline state, starch (Fig. 2b) has a distinct peak around $2\theta = 17.65^\circ$ and a low-intensity, broad peak between 21.85° and 24.25° (Todica et al., 2016). The amorphous state decreased, and a small amount of crystallinity was generated when PAM and starch were combined, resulting in new sharper peaks at 2θ of around 31.7° and 45.6° (Fig. 2c). The intensity of these peaks is higher than pure PAM and starch, which indicates that the polymers were properly incorporated. The broad peak of PAM was slightly shifted from 25° to 21.2° by the addition of starch (Singh & Mahto, 2017). In the XRD examination of GQDs (Fig. 2d), the hexagonal lattice shape is shown by two separate peaks around 2θ positions of 38.4° and 44.65° . GQDs' crystalline nature is confirmed by this distinctive pattern, which also offers important insights into their structural organization (Pooreesmaeil & Namazi, 2020). Due to the amorphous character of hydrogel, the PAM/Starch/GQDs nanocomposite's X-ray diffractogram (Fig. 2e) displays a large peak around $2\theta = 13^\circ$ – 25° . The strong peaks around $2\theta = 31.58^\circ$ and 45.4° reveal

that the amorphous matrix of PAM/Starch hydrogel is decreased upon the addition of GQDs, leading to crystalline nanocomposites. These peaks have a greater intensity than the spectra of PAM/Starch, which suggests that the PAM/Starch nanocomposite with GQDs was correctly comprised (Ostovar, Pourmadiadi & Zaker, 2023). There are no crystal-like peaks of QC observed in the CMC/starch/Cu-CQDs@QC XRD spectrum, reflecting that it is encapsulated within the nanocomposite's voids, improving nanocarrier crystallization. A recent study demonstrates that QC exhibits notable peaks from 12° to 25° , providing its crystalline form. On the other hand, the incorporation of QC into PAM/Starch/GQDs slightly shifted the diffraction peaks of PAM-Starch/GQDs, from 31.58° to 31.42° and 45.4° to 45.22° . As illustrated by Fig. 2f, this shift is beneficial for drug delivery applications since the model drug is more soluble in its non-crystalline form than in its crystal shape (M. Najafi et al., 2024).

3.3. Evaluation of structural morphology and size

FE-SEM examination was applied for looking at the morphology and surface properties of PAM/Starch/GQDs@QC nanocarriers. A mostly well-dispersed and semi-spherical particle configuration is constantly seen in minuscule pictures (Fig. 3) under different enlargements, which is extremely beneficial for DDSs. The typical size range of these nanocarriers is 42.68–58 nm. Significantly, the homogeneous surface of the nanocarriers demonstrated remarkable drug compliance (Masnavi et al., 2024). The distribution of nanocarrier particle sizes was investigated

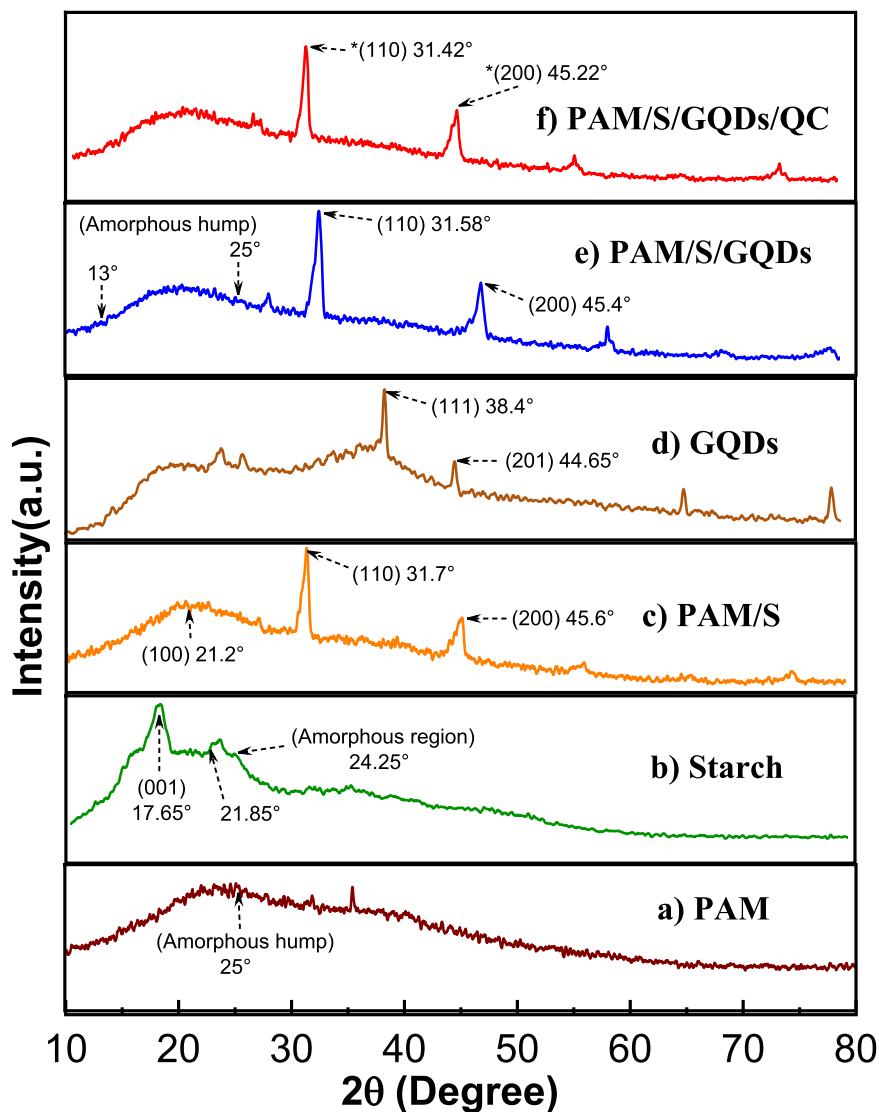


Fig. 2. The diffraction profiles of: a) PAM, b) Starch, c) PAM/Starch, d) GQDs, e) PAM/Starch/GQDs nanocomposite, and f) PAM/Starch/GQDs@QC nanocarrier (*Shifted due to QC loading).

utilizing the DLS technique. The mean size of the particles is 134.16 nm, dispersed in a spectrum between 82.33 nm and 193.48 nm, as seen in Fig. 4.a. It also means that a surfactant (SPAN 80) with a protective barrier and coating of hazelnut oil should be developed surrounding the nanocarrier, which would cause the particle size to increase. This finding is further corroborated by FE-SEM pictures. The homogeneous particle size dispersion is highlighted through the minimal Polydispersity Index (PDI) of 0.28, which guarantees stability within a colloidal medium. Surface charges were measured by zeta potential assessment. The stability of nanocarriers is shown by surface charges, which show electrostatic attraction and repulsion between them. Fig. 4.b displays the value of the zeta potential, where the surface charge for PAM/Starch/GQDs@QC nanocarriers was measured to be an average of + 53.3 mV. The dispersion of these nanocarriers is stable since this value is greater than the critical value. It is crucial to maintain an elevated zeta potential since low numbers might cause nanoparticle formation and aggregation. Large surface charges are produced by high zeta potentials, helping NPs disperse via electrostatic forces. The Zeta potential and DLS assessment findings for the novel nanocarriers are displayed in Table 1. In accordance with the outcomes of previous nanocarriers, the elevated surface charge revealed that the nanocarrier generated by this investigation is within the proper range of values. Therefore, the calculated

distribution of particle size and zeta potential provides the required efficacy for the planned sustained administration of QC (M. Najafi et al., 2024; Karami, Pourmadadi, Abdouss & Kalaei, 2025).

3.4. Evaluation of QC EE % and LE %

Drug entrapment efficiency (EE) and loading efficiency (LE) are two crucial factors that are measured using UV-visible spectrophotometry at 370 nm for a comprehensive assessment of DDSs. These values are computed using Eqs. (1) and 2. As previously demonstrated, the bioavailability of QC is significantly diminished due to its relatively low solubility in water. Employing nanocarriers to boost medication absorption and TDD to malignant tumors is one way to address this issue and can greatly improve the effectiveness of cancer therapy (Caro et al., 2022). We determined the EE and LE for PAM/Starch@QC hydrogel-carrier without GQDs and PAM/Starch/GQDs@QC hydrogel-nanocarrier with GQDs within this particular situation to evaluate the effect of including carbon-based NPs into the polymeric matrix. Our computations for PAM/Starch@QC revealed EE and LE of 75 % and 33.5 %, respectively (refer to Table 2). Nevertheless, we noticed an improvement after adding GQDs, with EE and LE of 89 % and 48 %, respectively. Strong interactions between the different parts of the

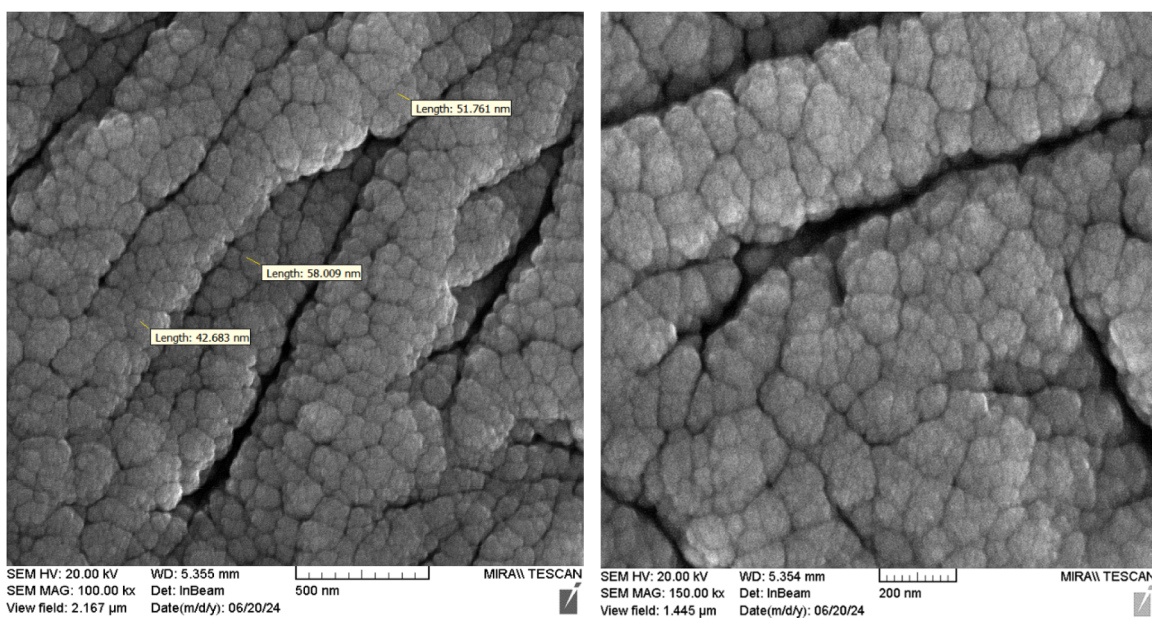


Fig. 3. The FE-SEM micrographs of freeze-dried PAM/Starch/GQDs@QC that depict the nanocarriers are displayed. Two distinct magnifications at 500 and 200 nm are illustrated by the images on the left and right, respectively.

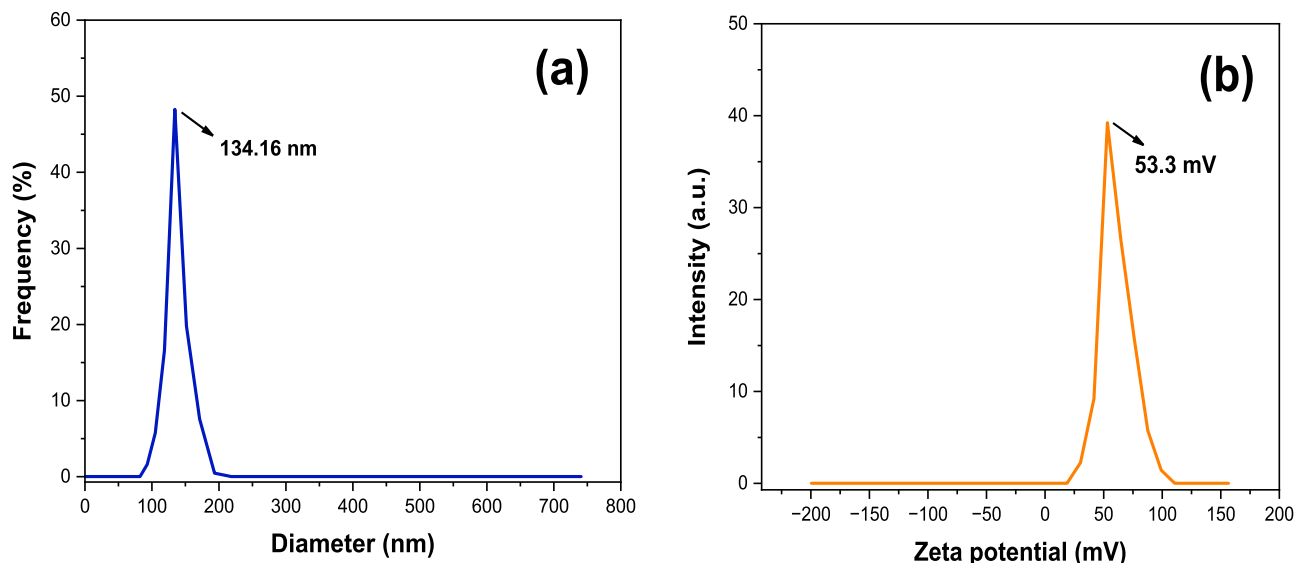


Fig. 4. The range of particle size ascertained through Dynamic Light Scattering (DLS) examinations is displayed in the plot on the left (a). Concurrently, the zeta potential intensity spectrum on the right side (b) reveals unique characteristics of the PAM/Starch/GQDs@QC nanocarriers.

nanocarrier are responsible for the increase in LE and EE that occurs when carbon-based NPs are incorporated. These interactions include the $C=O$ groups of GQDs nanoparticles, NH_2 groups of PAM, and the $O-H$ groups of starch and quercetin. When these powerful interactions come together, a network of interconnections is formed that is ideal for drug loading (M. Najafi et al., 2024). Additionally, enhancing QC encapsulation and loading requires the extraordinarily large surface area of GQDs. By expanding the quantity of area accessible during interactions among the QC and nanocomposite's constituents, this enormous surface area further improves the efficacy of drug insertion.

Table 3, Scheme 1

3.5. Kinetic of QC release

Statistical analysis of the release data at two pH values (under tumor

environment (pH 5.4) and normal conditions (pH 7.4)) has been used to perform kinetic assessments. To determine the major mechanism of QC release, drug release data from the developed PAM/Starch/GQDs@QC nanocarrier was fitted to zero and first-order, Hixson-Crowell, Korsmeyer-Peppas, and Higuchi kinetic models. As mentioned earlier, the curve fitting model was used to evaluate the release behavior of QC; R-squared values were investigated; the results are displayed in Tables 4 and Fig. 5. According to Table 4, the Korsmeyer-Peppas model had the highest R^2 value when compared to other models ($R^2 = 0.999$ for pH 5.4 and $R^2 = 0.994$ for pH 7.4), with n values ranging from 0.47 to 0.8 in both acidic and alkaline environments. This suggests that the drug release pattern is governed by a non-Fickian diffusion mechanism, indicating that both diffusion and matrix relaxation contribute to the release process. (Askarizadeh et al., 2023). The Higuchi model also showed a fair correlation, with R^2 values of 0.9986 for pH 5.4 and

Table 1

Comparing the size and surface charge of the innovative nanocarriers (* Particle size comparison based on FE-SEM analysis).

Nanocarrier	DLS (nm)	Zeta potential (mV)	Size (nm)*	Reference
Aga/GQDs/ α -Fe ₂ O ₃ @QC	279.04	52.8	~ 100–250	(M. Najafi et al., 2024)
PAA/Aga/ZnONPs/QC	207 and 321	-15.6 and -18.6	-	(Ahmadi et al., 2023)
CS/CMC/GQDs/ZnO@QC	219.38	- 53	-	(Ostovar, Pourmadadi & Zaker, 2023)
CMC/Starch/Cu-CQDs@QC	151.57	+ 38.8	-	(M. Najafi et al., 2024)
CMC/Fe ₃ O ₄ @SiO ₂ /QC	151.6	44.49	41.2 and 95.4	(Eshaghi, Pourmadadi, Rahdar & Díez-Pascual, 2022)
PAA/PVP/MoS ₂ @5-FU	315	-33.5	~ 100–300	(Pourmadadi et al., 2024)
CS/Aga/TiO ₂ -CQDs@5-FU	134.16	-38.63	500 nm to 1 μ m	(Masnavi et al., 2024)
CS/ γ Al ₂ O ₃ /GQDs@QC	523.4	11.06	19.8–240.4	(Karami, Pourmadadi, Abdouss & Kalaee, 2025)
PEG/CMS/ γ -Al ₂ O ₃ /CUR	193	+35.43	150–200	(Adeli et al., 2024)
PAM/Starch/GQDs@QC	134.16	+ 53.3	42.68–58	Current study

Table 2

The influence of GQDs on hydrogel-carriers consists of QC's encapsulation and loading efficiency.

Efficiency	PAM/Starch@QC	PAM/Starch/GQDs@QC	Effect of
Encapsulation (%)	75	89	+14
Loading (%)	33.5	48	+14.5

0.9908 for pH 7.4, although these were lower than those obtained with the Korsmeyer–Peppas model. This indicates that diffusion contributes partially to the release mechanism, particularly in the early stages, but does not fully explain the release behavior observed in this system.

This release method is consistent with the component relations and the generated nanocarrier structure. The structural integrity of the nanocarrier is preserved and prevented from dissolving by the chemical and physical interactions between the drug and the nanocomposite components. As a result, the release profile's main focus is diffusion, which is in line with the previously published data.

3.6. In vitro release of medication study

The pH-sensitive quercetin liberation from the PAM/Starch/GQDs@QC nanocarrier was examined in vitro using a dialysis technique under acidic and physiological conditions. It's also important to note that these tests were conducted at 37 °C, which is the usual body

temperature. The pH levels about 5.4 and 7.4 were chosen to correspond to tumor circumstances and normal blood pH, respectively. The quantity at pH 7.4 went down gradually until it decreased to 8 %, but Fig. 6 shows a huge release (16 %) in the initial 3 h of the full liberation period at pH 5.4. Release rates of QC at 12, 24, 48, 72, and 96 h were 35 %, 49 %, 68 %, 86 %, and 97 % in the malignant tissues (pH 5.4), respectively. On the other hand, the drug showed much-reduced release rates under normal metabolic environments (pH 7.4), with 21 %, 28 %, 37 %, 42 %, and 51 % liberation within suitable moment periods. Our results highlight the nanocarrier's long-term and sustained release characteristics, which were especially noticeable throughout the 96-h period. Because the GQDs are integrated into the matrix of the polymers, which creates an amorphous network of hydrogen bonds and van der Waals interactions, they lose their crystallinity. The cohesiveness of the nanocomposite is enhanced by these weak pressures. A controlled release pattern is also shown by the nanocomposite's QC release profile. Instead of being released suddenly, the drug is released gradually over time. Preserving effective medication concentrations and perhaps decreasing side effects are two advantages of this controlled release (Karami, Pourmadadi, Abdouss & Kalaee, 2025). In a recent investigation by Ostovar et al. (Ostovar, Pourmadadi & Zaker, 2023), a CS/CMC/GQD/ZnO nanocomposite was used to administer the anticancer medication QC and explore their drug delivery application. Their synthesized nanocomposite exhibited a slower release pattern, reaching 82 % release in the cancerous environment after 72 h, whereas in our case, this amount was 86 %.

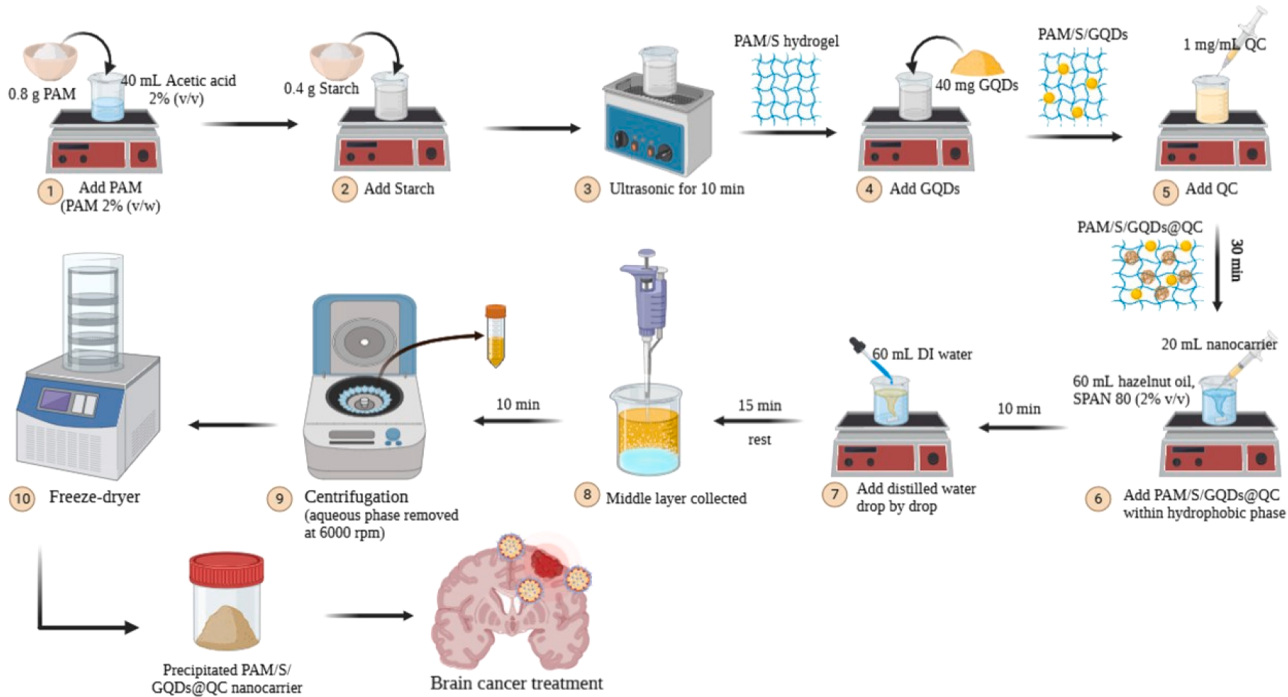
3.7. MTT assay assessment

The L929 cell lines were utilized for assessing the biocompatibility of PAM, PAM/Starch, PAM/Starch/GQDs, PAM/Starch/GQDs@QC, and free drug (QC). The 100 % viability of cells in PAM and PAM/Starch hydrogels makes them biocompatible, as shown in Fig. 7. Cell viability slightly decreased with the inclusion of GQDs, verifying the PAM/Starch/GQDs nanocomposite's biocompatibility with 98 % cell viability. Furthermore, PAM/Starch/GQDs@QC nanocarriers do not cause significant harm to L929 cell types, and 95 % of the cells were found to be alive. This outcome is crucial because it demonstrates that the harmful effects of the produced nanocarriers are diminishing. Additionally, pure QC has a 13 % shorter life expectancy than the nanocomposite containing QC for normal cells (L929), highlighting the efficacy of those developed DDSs. Examined on U-87 MG cell types, cellular toxicity on malignant cells demonstrates the nanocarrier's capacity for inhibiting brain tumor growth and triggering their death. Adding starch resulted in a minor reduction of cell survival in the PAM hydrogel (97 %), while the addition of GQDs to PAM/Starch hydrogel caused a 91 % decrease in its viability. After the drug was loaded into the nanocomposites, the development rate of U-87 MG cancer cells reached 56 %, indicating 7 % more inhibitory effects than free QC. This suggests that the anti-cancer features of drug-containing nanocomposites are far superior and more targeted than those of free QC. These findings confirmed the minimal toxicity of these nanocarriers on healthy cells and their substantial influence on the treatment of brain tumors (Masnavi et al., 2024).

Table 3

A few recently developed pH-sensitive QC-loaded delivery methods in contrast to the ongoing study.

Nanocarrier for QC delivery	Drug encapsulation efficiency (%)	Drug loading efficiency (%)	Target organ	Reference
Aga/GQDs/ α -Fe ₂ O ₃ @QC	86.25	47	Liver	(M. Najafi et al., 2024)
PAA/Aga/ZnONPs/QC	87.25	47.5	Breast	(Ahmadi et al., 2023)
CS/CMC/GQDs/ZnO@QC	87.5	46.75	Brain	(Ostovar, Pourmadadi & Zaker, 2023)
CMC/Starch/Cu-CQDs@QC	86.25	47	Brain	(M. Najafi et al., 2024)
CMC/Fe ₃ O ₄ @SiO ₂ /QC	47.25	88.5	Lung	(Eshaghi, Pourmadadi, Rahdar & Díez-Pascual, 2022)
CS/ γ Al ₂ O ₃ /GQDs@QC	87	46.75	Lung	(Karami, Pourmadadi, Abdouss & Kalaee, 2025)
PAM/Starch/GQDs@QC	89	48	Brain	Current study



Scheme 1. A graphic illustration of the dual-phase emulsification technique used for synthesizing a PAM/S/GQDs@QC nanocarrier.

Table 4
Kinetic models of drug release.

Kinetic framework	pH	Equation	R-squared
Zero-order	5.4	$C_t = 1.0009 t + 11.751$	0.9249
	7.4	$C_t = 0.5234 t + 5.9816$	0.8932
First-order	5.4	$\ln(1 - \frac{C_t}{C_\infty}) = -0.032 t + 0.0083$	0.9585
	7.4	$\ln(1 - \frac{C_t}{C_\infty}) = -0.0072 t - 0.0578$	0.9407
Higuchi	5.4	$\frac{C_t}{C_\infty} = 0.0991 \sqrt{t} + 0.0047$	0.9986
	7.4	$\frac{C_t}{C_\infty} = 0.0453 \sqrt{t} + 0.0536$	0.9908
Korsmeyer-Peppas	5.4	$\ln(\frac{C_t}{C_\infty} \times 100) = 0.4941 \ln(t) - 2.2818$	0.9991
	7.4	$\ln(\frac{C_t}{C_\infty} \times 100) = 0.4113 \ln(t) - 2.5854$	0.994
Hixon-Crowell	5.4	$\sqrt[3]{1 - \frac{C_t}{C_\infty}} = 0.0068 t + 0.0246$	0.9886
	7.4	$\sqrt[3]{1 - \frac{C_t}{C_\infty}} = 0.0022 t + 0.02$	0.926

4. Conclusion

Most widely utilized QC delivery methods possess a restricted drug loading capacity and often have unfavorable effects. The present study focused on creating a novel hydrogel-based nanocomposite containing PAM, starch, and GQDs through a dual-phase emulsion technique (W/O/W) for improving the effectiveness of QC toward U-87 MG (brain cells that are cancerous). The outcome of the PAM and starch combination was a strong and biocompatible hydrogel. GQDs nanoparticles were added to the polymer matrix to increase the hydrogel's mechanical qualities and biocompatible DDS. Drug transport inside the body may be safely and effectively tracked with GQDs. All things considered, this novel nanocarrier technology is a major step forward in solving medication release issues, leading to safer and more effective cancer therapy alternatives. The PAM/Starch/GQDs@QC nanocarrier and its constituents were thoroughly characterized and morphologically examined utilizing methods consisting of FTIR, XRD, FE-SEM, DLS, and Zeta

potential. The particle size distribution of the nanocarriers commonly falls within the range of 42.68 to 58 nm, which contributes to their high surface area, improved drug loading capacity, and favorable bio-distribution in tumor tissues. The Polydispersity Index (PDI) value of 0.28 demonstrates a tight size distribution among the particles, implying consistent dispersion and stability in the colloidal environment. The zeta potential of the PAM/Starch/GQDs@QC nanocarriers was found to be approximately +53.3 mV, indicating a strongly positive surface charge that enhances electrostatic repulsion and reduces the likelihood of particle aggregation.

The findings of the research showed an EE of 89 % and a LE of 48 %. The Korsmeyer-Peppas model showed the best fit to our release data ($R^2 = 0.999$ at pH 5.4 and $R^2 = 0.994$ at pH 7.4), suggesting that the release kinetics followed a non-Fickian diffusion mechanism. This was further supported by the slope of the fitted line ($0.45 < n < 0.89$), confirming the anomalous transport behavior of QC. As demonstrated by FTIR analyses, it's mostly caused by the many bonds of hydrogen that are formed among the PAM and starch (peaks at approximately 3263–3632 cm^{-1}) as well as between the GQDs and the configuration of the polymer. Because of the robust structure these hydrogen bonds give the nanocomposite, drug loading, and controlled release are enhanced. Overall, the drug release assessment confirmed that, at the conclusion of the 96 h evaluation, the amount of drug diffused in the tumor-like medium (pH 5.4) surpassed that in the normal tissue model (pH 7.4) by approximately 46 %. This selective delivery behavior highlights the potential of the system to provide more localized and effective therapeutic action, with reduced exposure to healthy cells. MTT assay results on the normal cells (L929) showed that the PAM/Starch/GQDs@QC nanocarrier exhibited approximately 13 % lower cytotoxicity compared to free QC, while on the cancerous cells (U-87 MG), it showed about 7 % higher cytotoxicity. This significant reduction in toxicity toward normal cells confirms its high biocompatibility. Consequently, the PAM/Starch/GQDs@QC nanocarrier is regarded as a superior platform for encapsulating QC, leading to improved controlled release, drug circulation time, and bioavailability within the body. This nanocarrier demonstrated an impressive anticancer influence on brain cancerous cells in addition to minimal toxicity on healthy cells, resulting in a potent therapeutic carrier for an uncommon disease like brain cancer. For brain treatment

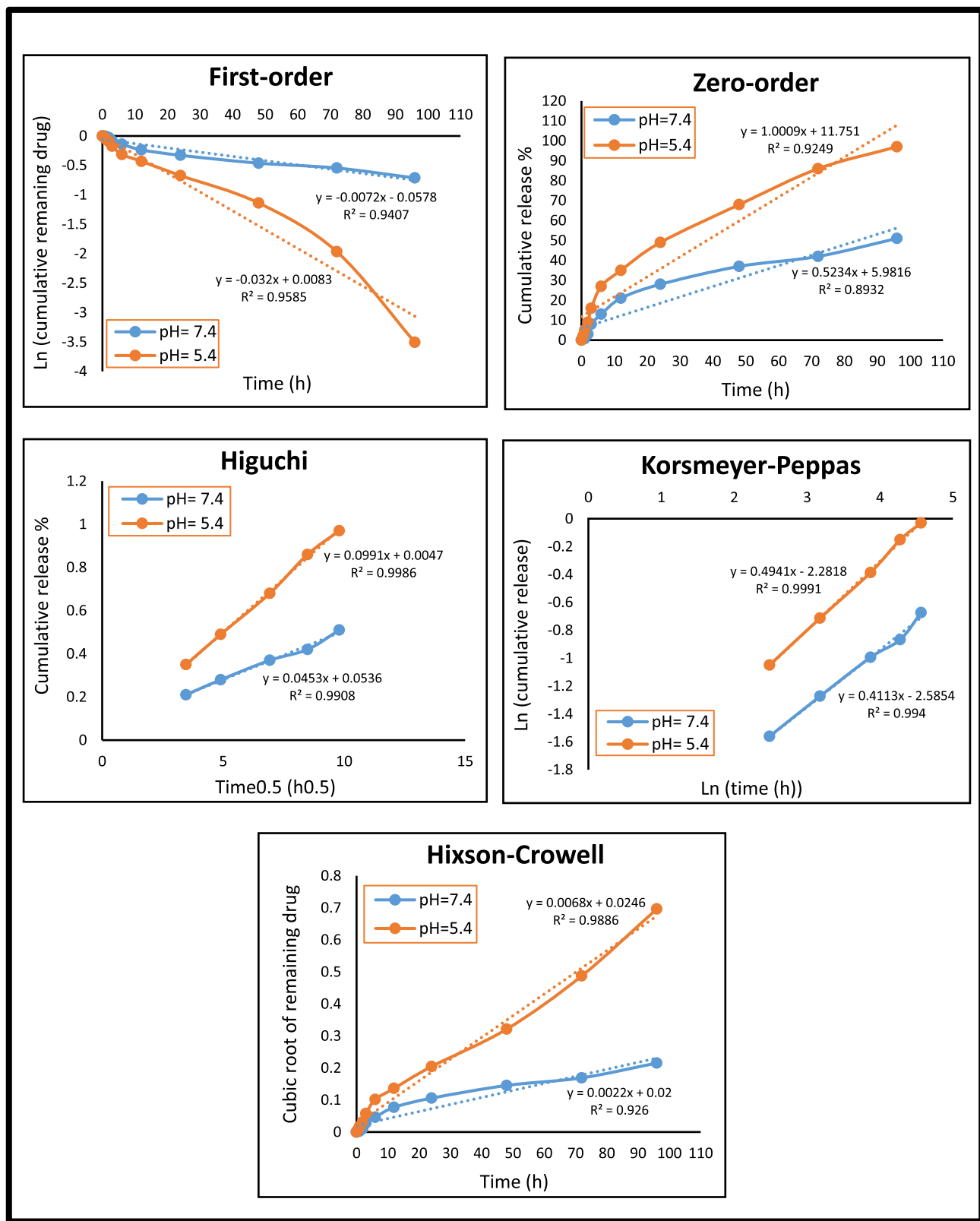


Fig. 5. The graphs show fitted data with different kinetic models of QC release.

purposes, this nanocarrier suggests a bright prospect for the coupling of co-biopolymers and carbon-based nano quantum dots.

5. Future perspective

The research investigates the appropriateness of nano-optimized DDSs while noting limits in generalization and their applicability to larger therapeutic contexts. Cellular intricacy and individual

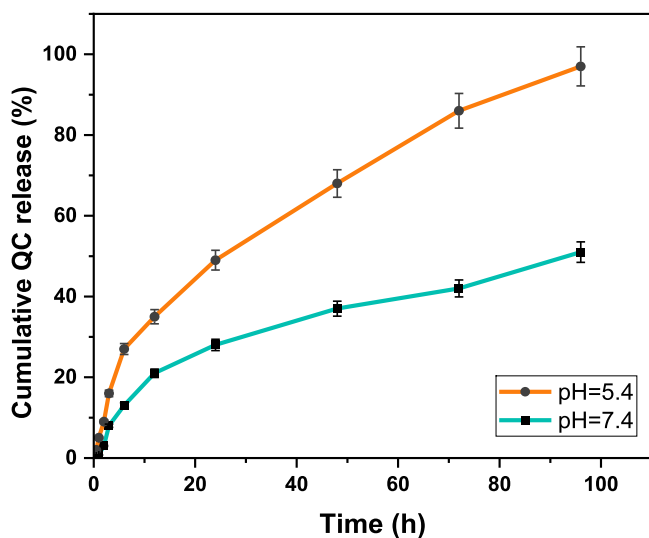


Fig. 6. The QC release pattern from the PAM/Starch/GQDs@QC nanocarrier is shown, along with how it behaves in both acidic and normal pH environments. Mean values \pm standard deviation across three replicates are used to report the data.

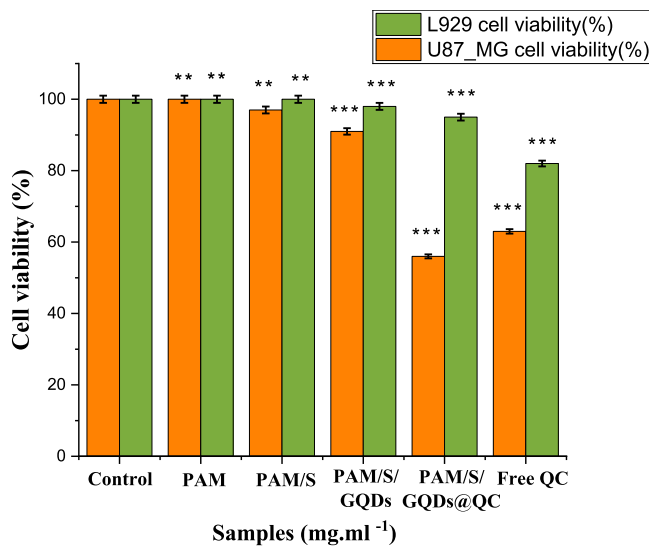


Fig. 7. Demonstrates the MTT assessment outcomes for both normal cells (L929) and cancer cells (U-87 MG), which were obtained during a 72-hour period. Three careful replications of the tests were conducted, so the results are presented as mean values together with the standard errors of the mean (SEM) that correspond to them. To find any notable variations among the analyzed specimens & the reference group, a comprehensive statistical investigation was undertaken. In particular, the ** and *** symbols imply significant levels below 0.01 ($p < 0.01$) and 0.001 ($p < 0.001$), respectively.

heterogeneity give difficulties for this study, even though it offers insightful information on medicine delivery via nanotechnology. Future research may investigate the efficacy of alternative chemotherapy agents in conjunction with the drug-loaded nanocomposite hydrogel, rather than utilizing QC. Further investigations may also assess the anticancer effects of this PAM/Starch/GQDs@QC nanocarrier on a wider spectrum of cancer cell types originating from various body tissues to better understand its broader therapeutic applicability. Moreover, integrating thermosensitive or magnetosensitive properties into the nanocomposite structure could enable controlled and environment-responsive drug release, offering valuable insights into the system's behavior under varying physiological conditions and potentially

enhancing its clinical performance. In addition, we recommended conducting animal studies to evaluate the biocompatibility and potential toxicity of the nanocarriers in various body organs.

CRediT authorship contribution statement

Pardis Ordoukhani: Writing – original draft, Visualization, Software, Resources, Methodology, Investigation, Funding acquisition, Formal analysis, Data curation. **Mehrab Pourmadadi:** Writing – review & editing, Writing – original draft, Visualization, Validation, Supervision, Software, Resources, Project administration, Methodology, Investigation, Funding acquisition, Formal analysis, Conceptualization. **Majid Abdouss:** Supervision, Methodology, Investigation, Formal analysis, Data curation.

Declaration of competing interest

The authors declare that they have no known competing financial interests or personal relationships that could have appeared to influence the work reported in this paper.

Data availability

Data will be made available on request.

References

- Adeli, F., Pourmadadi, M., Abdouss, M., Rahdar, A., Fathi-karkan, S., Samandari, S. S., & Díez-Pascual, A. M. (2024). Controlled curcumin delivery via carboxymethyl starch-modified gamma alumina nanoparticles in a polyethylene glycol-based hydrogel. *Journal of applied polymer science*, 141, Article e55946.
- Ahmadi, H., Pourmadadi, M., Abdouss, M., Rahdar, A., & Díez-Pascual, A. M. (2023). Formulation of double nanoemulsions based on pH-sensitive poly acrylic acid/agarose/ZnO for quercetin controlled release. *Journal of molecular liquids*, 391, Article 123363.
- Almatroodi, S. A., Alsahli, M. A., Aljohani, A. S. M., Alhumaydhi, F. A., Babiker, A. Y., Khan, A. A., & Rahmani, A. H. (2022). Potential therapeutic targets of resveratrol, a plant polyphenol, and its role in the therapy of various types of cancer. *Molecules (Basel, Switzerland)*, 27, 2665.
- Arcos, D., & Vallet-Regi, M. (2013). Bioceramics for drug delivery. *Acta materialia*, 61, 890–911.
- Askarizadeh, M., Esfandiari, N., Honarvar, B., Sajadian, S. A., & Azdarpour, A. (2023). Kinetic modeling to explain the release of medicine from drug delivery systems. *ChemBioEng Rev*, 10, 1006–1049.
- Atanasov, A. G., Zotchev, S. B., Dirsch, V. M., & Supuran, C. T. (2021). Natural products in drug discovery: Advances and opportunities. *Nature reviews. Drug discovery*, 20, 200–216.
- Avval, M. E., Moghaddam, P. N., & Fareghi, A. R. (2013). Modification of starch by graft copolymerization: A drug delivery system tested for cephalaxin antibiotic. *Starch-Stärke*, 65, 572–583.
- Azari, A., Nabizadeh, R., Mahvi, A. H., & Nasser, S. (2022). Integrated Fuzzy AHP-TOPSIS for selecting the best color removal process using carbon-based adsorbent materials: Multi-criteria decision making vs. systematic review approaches and modeling of textile wastewater treatment in real conditions. *International journal of environmental analytical chemistry*, 102, 7329–7344.
- Azeem, M., Hanif, M., Mahmood, K., Ameer, N., Chughtai, F. R. S., & Abid, U. (2023). An insight into anticancer, antioxidant, antimicrobial, antidiabetic and anti-inflammatory effects of quercetin: A review. *Polymer Bulletin*, 80, 241–262.
- Brannon-Peppas, L., & Harland, R. S. (2012). *Absorbent polymer technology*. Elsevier.
- Builders, P. F., & Arhewoh, M. I. (2016). Pharmaceutical applications of native starch in conventional drug delivery. *Starch-Stärke*, 68, 864–873.
- Caro, C., Pourmadadi, M., Eshaghi, M. M., Rahmani, E., Shojaei, S., Paiva-Santos, A. C., Rahdar, A., Behzadnezh, R., García-Martín, M. L., & Díez-Pascual, A. M. (2022). Nanomaterials loaded with Quercetin as an advanced tool for cancer treatment. *Journal of Drug delivery science and technology*, 78, Article 103938.
- Elvira, C., Mano, J. F., San Roman, J., & Reis, R. L. (2002). Starch-based biodegradable hydrogels with potential biomedical applications as drug delivery systems. *Biomaterials*, 23, 1955–1966.
- Eshaghi, M., Mahdi, Pourmadadi, M., Rahdar, A., & Díez-Pascual, A. M. (2022). Novel carboxymethyl cellulose-based hydrogel with core-shell Fe3O4@ SiO2 nanoparticles for quercetin delivery. *Materials*, 15, 8711.
- Ghasemizadeh, H., Pourmadadi, M., Yazdian, F., Rashedi, H., Navaei-Nigjeh, M., Rahdar, A., & Díez-Pascual, A. M. (2023). Novel carboxymethyl cellulose-halloysite-polyethylene glycol nanocomposite for improved 5-FU delivery. *International journal of biological macromolecules*, 232, Article 123437.
- Goenka, S., Sant, V., & Sant, S. (2014). Graphene-based nanomaterials for drug delivery and tissue engineering. *J. Control. Release*, 173, 75–88.

- Haque, M. A., Kurokawa, T., Kamita, G., & Gong, J. P. (2011). Lamellar bilayers as reversible sacrificial bonds to toughen hydrogel: Hysteresis, self-recovery, fatigue resistance, and crack blunting. *Macromolecules*, *44*, 8916–8924.
- Henna, T. K., & Pramod, K. (2020). Graphene quantum dots redefine nanobiomedicine. *Mater. Sci. Eng. C*, *110*, Article 110651.
- Iannazzo, D., Pistone, A., Salamó, M., Galvagno, S., Romeo, R., Giofré, S. V., Branca, C., Visalli, G., & Di Pietro, A. (2017). Graphene quantum dots for cancer targeted drug delivery. *International journal of pharmaceutics*, *518*, 185–192.
- Iannazzo, D., Celesti, C., & Espriu, C. (2021). Recent advances on graphene quantum dots as multifunctional nanoplatforms for cancer treatment. *Biotechnology journal*, *16*, Article 1900422.
- Ishisaka, A., Ichikawa, S., Sakakibara, H., Piskula, M. K., Nakamura, T., Kato, Y., Ito, M., Miyamoto, K., Tsuji, A., & Kawai, Y. (2011). Accumulation of orally administered quercetin in brain tissue and its antioxidative effects in rats, Free Radic. *Biologie et médecine*, *51*, 1329–1336.
- S.F. Jokandan, M.Y. Badi, A. Esrafili, A. Azari, H. Tarhandeh, M. Kermani, Investigation of the efficiency of powder activated carbon magnetized with Fe3O4 nanoparticles in the removal of catechol from aqueous solutions by response surface methodology., (2019).
- Kandow, C. E., Georges, P. C., Jamney, P. A., & Beningo, K. A. (2007). Polyacrylamide hydrogels for cell mechanics: Steps toward optimization and alternative uses. *Methods in cell biology*, *83*, 29–46.
- Karami, M., Pourmadadi, M., Abdouss, M., & Kalaei, M. (2025). Synthesis, characterization, and In vitro analysis of a chitosan/gamma alumina/graphene quantum dots/bio-hydrogel for quercetin delivery to lung cancer cells. *BioNanoScience*, *15*, 1–19.
- Kazemi, S., Pourmadadi, M., Yazdian, F., & Ghadami, A. (2021). The synthesis and characterization of targeted delivery curcumin using chitosan-magnete-reduced graphene oxide as nano-carrier. *International journal of biological macromolecules*, *186*, 554–562.
- Khodayari, H., Heydarinasab, A., Moniri, E., & Miralnagh, M. (2023). Synthesis and characterization of magnetic nanoparticles-grafted-hyaluronic acid/β-cyclodextrin as a novel pH-sensitive nanocarrier for targeted delivery of doxorubicin. *Inorganic chemistry communications*, *148*, Article 110366.
- Lesniak, M. S., & Brem, H. (2004). Targeted therapy for brain tumours. *Nature reviews. Drug discovery*, *3*, 499–508.
- Li, Z., Huang, J., & Wu, J. (2021). pH-sensitive nanogels for drug delivery in cancer therapy. *Biomaterials science*, *9*, 574–589.
- Lin, P., Ma, S., Wang, X., & Zhou, F. (2015). Molecularly engineered dual-crosslinked hydrogel with ultrahigh mechanical strength, toughness, and good self-recovery. *Advanced materials (Deerfield Beach, Fla)*, *27*, 2054–2059.
- Liu, Y., Xu, L.-P., Dai, W., Dong, H., Wen, Y., & Zhang, X. (2015). Graphene quantum dots for the inhibition of β amyloid aggregation. *Nanoscale*, *7*, 19060–19065.
- Liu, Y., Xu, L.-P., Wang, Q., Yang, B., & Zhang, X. (2017). Synergistic inhibitory effect of GQDs-tramiprosate covalent binding on amyloid aggregation. *ACS Chem. Neurosci.*, *9*, 817–823.
- Luo, Y.-L., Yuan, J.-F., Liu, X.-J., Xie, H., & Gao, Q.-Y. (2010). Self-assembled polyion complex micelles based on PVP-b-PAMPS and PVP-b-PDMAEMA for drug delivery. *Journal of bioactive and compatible polymers*, *25*, 292–304.
- Masnavi, M., Pourmadadi, M., Abdouss, M., Rahdar, A., Fathi-Karkan, S., & Pandey, S. (2024). Synthesis of nanocarrier based on Chitosan/agarose biopolymers containing carbon quantum dot doped titanium dioxide for targeted delivery of 5-fluorouracil for brain cancer treatment. *BioNanoScience*, *14*, 2264–2274.
- Miller, K. D., Ostrom, Q. T., Kruchko, C., Patil, N., Tihan, T., Cioffi, G., Fuchs, H. E., Waite, K. A., Jemal, A., & Siegel, R. L. (2021). Brain and other central nervous system tumor statistics, 2021. *CA: Cancer J. Clin.*, *71*, 381–406.
- Moulay, S., Bensacia, N., Garin, F., Fechete, I., & Boos, A. (2013). Polyacrylamide-based sorbents for the removal of hazardous metals. *Adsorption Science & Technology*, *31*, 691–709.
- Murthy, P. S. K., Mohan, Y. M., Sreeramulu, J., & Raju, K. M. (2006). Semi-IPNs of starch and poly (acrylamide-co-sodium methacrylate): Preparation, swelling and diffusion characteristics evaluation. *Reactive & functional polymers*, *66*, 1482–1493.
- Najafi, M., Khoddam, Z., Masnavi, M., Pourmadadi, M., & Abdouss, M. (2024a). Physicochemical and in vitro characterization of agarose based nanocarriers incorporated with graphene Quantum dots/α-Fe2O3 for targeted drug delivery of Quercetin to liver cancer treatment. *Materials chemistry and physics*, *320*, Article 129333.
- Najafi, M., Pourmadadi, M., Abdous, M., Rahdar, A., & Pandey, S. (2024b). Formulation of double nanoemulsions based on pH-sensitive carboxymethyl cellulose/starch copper doped carbon quantum dots for quercetin controlled release. *Journal of molecular liquids*, *400*, Article 124543.
- Nance, E., Pun, S. H., Saigal, R., & Sellers, D. L. (2022). Drug delivery to the central nervous system. *Nature reviews. Materials*, *7*, 314–331.
- Narasimhan, B., Peppas, N. A., & Park, K. (1997). *Controlled release: Challenges and strategies* (p. 529). Washington, DC: ACS.
- Nathiya, S., Durga, M., & Devasena, T. (2014). Quercetin, encapsulated quercetin and its application—A review. *Analgesia*, *10*, 20–26.
- Nozhat, Z., Wang, S., Mushtaq, A., Deng, T., Iqbal, M. Z., & Kong, X. (2024). Temozolomide loaded Fe3O4@ SiO2 nanoparticles for MR-imaging directed synergistic therapy of glioblastoma multiforme in vitro. *Materials Today Communications*, *38*, Article 108289.
- Ostovar, S., Pourmadadi, M., & Zaker, M. A. (2023). Co-biopolymer of chitosan/carboxymethyl cellulose hydrogel improved by zinc oxide and graphene quantum dots nanoparticles as pH-sensitive nanocomposite for quercetin delivery to brain cancer treatment. *International journal of biological macromolecules*, *253*, Article 127091.
- Ostovar, S., Pourmadadi, M., Shamsabadipour, A., & Mashayekh, P. (2023). Nanocomposite of chitosan/gelatin/carbon quantum dots as a biocompatible and efficient nanocarrier for improving the Curcumin delivery restrictions to treat brain cancer. *International journal of biological macromolecules*, *242*, Article 124986.
- Ostrom, Q. T., Gittleman, H., Liao, P., Rouse, C., Chen, Y., Dowling, J., Wolinsky, Y., Kruchko, C., & Barnholtz-Sloan, J. (2014). CBTRUS statistical report: Primary brain and central nervous system tumors diagnosed in the United States in 2007–2011. *Neuro-Oncology*, *16*, iv1–iv63.
- Parvaneh, S., Pourmadadi, M., Abdouss, M., Pourmousavi, S. A., Yazdian, F., Rahdar, A., & Díez-Pascual, A. M. (2023). Carboxymethyl cellulose/starch/reduced graphene oxide composite as a pH-sensitive nanocarrier for curcumin drug delivery. *International journal of biological macromolecules*, *241*, Article 124566.
- Parvathy, P. C., & Jyothi, A. N. (2012). Synthesis, characterization and swelling behaviour of superabsorbent polymers from cassava starch-graft-poly (acrylamide). *Starch-Stärke*, *64*, 207–218.
- Peppas, N. A., & Langer, R. (1994). New challenges in biomaterials. *Science (80-.)*, *263*, 1715–1720.
- Peppas, N. A. (1986). *Hydrogels in medicine and pharmacy*. Boca Raton, FL: CRC press.
- Peppas, N. A. (1997). Hydrogels and drug delivery. *Current Opinion in Colloid & Interface Science*, *2*, 531–537.
- Pooresmaili, M., & Namazi, H. (2020). pH-sensitive ternary Fe3O4/GQDs@ G hybrid microspheres; synthesis, characterization and drug delivery application. *Journal of Alloys and Compounds*, *846*, Article 156419.
- Pourmadadi, M., Abdouss, M., Eshaghi, M. M., Ostovar, S., Mohammadi, Z., Sharma, R. K., Paiva-Santos, A. C., Rahmani, E., Rahdar, A., & Pandey, S. (2023). Innovative nanomaterials for cancer diagnosis, imaging, and therapy: Drug delivery applications. *Journal of Drug delivery science and technology*, *82*, Article 104357.
- Pourmadadi, M., Abdouss, M., Mazinani, S., Behzadmehr, R., Rahdar, A., & Aboudzadeh, M. A. (2024). Hybrid nanocarriers based on polyacrylic acid, polyvinyl pyrrolidone, and molybdenum disulfide for enhanced 5-fluorouracil delivery in lung cancer therapy. *Inorganic chemistry communications*, *159*, Article 111749.
- Pourmadadi, M., Ahmadi, M., & Yazdian, F. (2023). Synthesis of a novel pH-responsive Fe3O4/chitosan/agarose double nanoemulsion as a promising nanocarrier with sustained release of curcumin to treat MCF-7 cell line. *International journal of biological macromolecules*, *235*, Article 123786.
- Power, E. A., Rechberger, J. S., Gupta, S., Schwartz, J. D., Daniels, D. J., & Khutia, S. (2022). Drug delivery across the blood-brain barrier for the treatment of pediatric brain tumors—An update. *Advanced drug delivery reviews*, *185*, Article 114303.
- Rahmani, E., Pourmadadi, M., Zandi, N., Rahdar, A., & Baino, F. (2022). pH-responsive PVA-based nanofibers containing GO modified with Ag nanoparticles: Physico-chemical characterization, wound dressing, and drug delivery. *Micromachines*, *13*, 1847.
- Ratner, B. D. (1976). Hydrogels for medical and related applications. *ACS symp. ACS. P. Chapter-1*.
- RezaeiKalantary, R., JonidiJafari, A., Kakavandi, B., Nasser, S., Ameri, A., & Azari, A. (2014). Adsorption and magnetic separation of lead from synthetic wastewater using carbon/iron oxide nanoparticles composite. *J. Maz. Univ. Med. Sci.*, *24*, 172–183.
- Saeed, N., Khan, M. R., & Shabbir, M. (2012). Antioxidant activity, total phenolic and total flavonoid contents of whole plant extracts *Torilis leptophylla* L. *BMC Complementary and Alternative Medicine*, *12*, 1–12.
- Setty, C. M., Deshmukh, A. S., & Badiger, A. M. (2014). Hydrolyzed polyacrylamide grafted maize starch based microbeads: Application in pH responsive drug delivery. *International journal of biological macromolecules*, *70*, 1–9.
- Shah, V., & Kochar, P. (2018). Brain cancer: Implication to disease, therapeutic strategies and tumor targeted drug delivery approaches. *Recent Patents on Anti-Cancer Drug Discovery*, *13*, 70–85.
- Shaik, S., Kummara, M. R., Poluru, S., Allu, C., Gooley, J. M., Kashay, C. R., & Subha, M. C. S. (2013). A green approach to synthesize silver nanoparticles in starch-co-poly (acrylamide) hydrogels by tridax procumbens leaf extract and their antibacterial activity. *International Journal of Carbohydrate Chemistry*, *2013*, Article 539636.
- Shala, A. L., Arduino, I., Salihu, M. B., & Denora, N. (2023). Quercetin and its nano-formulations for brain tumor therapy—Current developments and future perspectives for paediatric studies. *Pharmaceutics*, *15*, 963.
- Siegel, R. L., Miller, K. D., Wagle, N. S., & Jemal, A. (2023). Cancer statistics, 2023. *CA: A cancer journal for clinicians*, *73*, 17–48.
- Singh, R., & Mahto, V. (2017). Synthesis, characterization and evaluation of polyacrylamide graft starch/clay nanocomposite hydrogel system for enhanced oil recovery. *Petroleum science*, *14*, 765–779.
- Su, X., Mahalingam, S., Edrisringhe, M., & Chen, B. (2017). Highly stretchable and highly resilient polymer-clay nanocomposite hydrogels with low hysteresis. *ACS Applied Materials & Interfaces*, *9*, 22223–22234.
- Sujka, M., Pankiewicz, U., Kowalski, R., Nowosad, K., & Noszczyk-Nowak, A. (2018). Porous starch and its application in drug delivery systems. *Polimery w medycynie*, *48*.
- Sung, H., Ferlay, J., Siegel, R. L., Laversanne, M., Soerjomataram, I., Jemal, A., & Bray, F. (2021). Global cancer statistics 2020: GLOBOCAN estimates of incidence and mortality worldwide for 36 cancers in 185 countries. *Cancer Journal for Clinicians*, *71*, 209–249.
- Tade, R. S., & Patil, P. O. (2020). Theranostic prospects of graphene quantum dots in breast cancer. *ACS Biomater. Sci. Eng.*, *6*, 5987–6008.
- Todica, M., Nagy, E. M., Niculaescu, C., Stan, O., Cioica, N., & Pop, C. V. (2016). XRD investigation of some thermal degraded starch based materials. *Journal of Spectroscopy*, *2016*, Article 9605312.
- Torres-Figueroa, A. V., Pérez-Martínez, C. J., del Castillo-Castro, T., Bolado-Martínez, E., Corella-Madueño, M. A. G., García-Alegria, A. M., Lara-Ceniceros, T. E., & Armenta-Villegas, L. (2020). Composite hydrogel of poly (acrylamide) and starch as potential

- system for controlled release of amoxicillin and inhibition of bacterial growth. *Journal of chemistry*, 2020, Article 5860487.
- Tsuruta, T. (1993). *Biomedical applications of polymeric materials*. CRC press.
- Vyas, S. P., & Khar, R. K. (2004). *Targeted & controlled drug delivery: Novel carrier systems*. CBS publishers & distributors.
- Wang, C., Wu, C., Zhou, X., Han, T., Xin, X., Wu, J., Zhang, J., & Guo, S. (2013). Enhancing cell nucleus accumulation and DNA cleavage activity of anti-cancer drug via graphene quantum dots. *Scientific reports*, 3, 2852.
- Zadeh, E. S., Ghanbari, N., Salehi, Z., Derakhhti, S., Amoabediny, G., Akbari, M., & Tokmedash, M. A. (2023). Smart pH-responsive magnetic graphene quantum dots nanocarriers for anticancer drug delivery of curcumin. *Materials chemistry and physics*, 297, Article 127336.
- Zhang, A., Zhang, Z., Shi, F., Ding, J., Xiao, C., Zhuang, X., He, C., Chen, L., & Chen, X. (2013). Disulfide crosslinked PEGylated starch micelles as efficient intracellular drug delivery platforms. *Soft matter*, 9, 2224–2233.
- Zhang, A. S., Ostrom, Q. T., Kruchko, C., Rogers, L., Peereboom, D. M., & Barnholtz-Sloan, J. S. (2017). Complete prevalence of malignant primary brain tumors registry data in the United States compared with other common cancers, 2010. *Neuro-Oncology*, 19, 726–735.
- Zoghi, M., Pourmadadi, M., Yazdian, F., Nigjeh, M. N., Rashedi, H., & Sahraeian, R. (2023). Synthesis and characterization of chitosan/carbon quantum dots/Fe₂O₃ nanocomposite comprising curcumin for targeted drug delivery in breast cancer therapy. *International journal of biological macromolecules*, 249, Article 125788.